Heat and Mass Transfer 38 (2001) 17–24 © Springer-Verlag 2001

Natural convection flow from a continuously moving vertical surface immersed in a thermally stratified medium

H. S. Takhar, A. J. Chamkha, G. Nath

Abstract Natural convection boundary layer flow over a continuously moving isothermal vertical surface immersed in a thermally stratified medium has been investigated here. The non-linear coupled partial differential equations governing the non-similar flow have been solved numerically using an implicit finite difference scheme. For small values of the streamwise distance the partial differential equations are solved by using a perturbation expansion procedure and also using the Shanks transformation. The results indicate that the thermal stratification significantly affects both the surface shear stress and the surface heat transfer. The buoyancy parameter and the Prandtl number increase significantly, both the surface shear stress and heat transfer. Also the buoyancy force gives rise to an overshoot in the velocity profile.

1 Introduction

Heat transfer processes by natural convection in a thermally stratified medium frequently occur in the natural environment and in many industrial and technical applications. Stratification is important in lakes, rivers and the sea, and in condensers of power plants and various industrial units. The natural convection flow over a heated vertical surface with uniform temperature immersed in an ambient fluid whose temperature increases linearly with height has been studied by Eichhorn [1], Chen and Eichhorn [2], and Venkatachala and Nath [3]. They solved the partial differential equations governing the flow by a using series solution method, the local non-similarity method and an implicit finite difference scheme, respectively. Kulkarni et al. [4] have obtained a similarity solution of the above problem.

The flow and heat transfer in the boundary layer induced by a surface moving with uniform or non-uniform velocity in an otherwise ambient fluid has many practical applications in manufacturing processes in industry. Sakiadis [5] was the first to study the flow due to a solid surface moving with a constant velocity in an ambient fluid. Since then several investigators [6–12] have considered various aspects of this problem such as the heat transfer with prescribed wall temperature or heat flux, mass transfer, non-uniform wall velocity, surface suction or blowing, effect of a magnetic field or (and) a parallel free stream velocity etc. In almost all the cases self-similar solutions were obtained. However, Jeng et al. [14] and Chiam [20] have studied the non-similar flow and heat transfer. In all the above studies the buoyancy forces resulting from the temperature differences in the fluid were neglected. Moutsoglou and Chen [22] have considered the effect of the buoyancy forces on the flow and heat transfer characteristics of the laminar boundary induced by an inclined, continuous flat surface that moves with a constant velocity in a fluid at rest. Subsequently, Ramachandran et al. [23] have presented the correlation equations for the local and average Nusselt numbers.

In this paper, we have investigated the flow and heat transfer characteristics of the steady laminar boundary layer induced by a vertical flat surface that moves with a constant velocity in a stable thermally stratified fluid at rest. We have considered the effect of the buoyancy forces which arise due to the temperature differences in the fluid. The coupled non-linear partial differential equations governing the flow have been solved numerically using an implicit finite-difference method [24]. For small values of the streamwise distance, the governing equations have been solved by using a perturbation expansion technique [25] along with the Shanks transformation [26]. For some particular cases, the results have been compared with the theoretical and experimental results of Tsou et al. [8], the theoretical results of Erickson et al. [6] and Moutsoglou and Chen [22] and the experimental results of Griffin and Throne [7].

Received on 1 February 2000

H. S. Takhar (✉)
Department of Engineering, Manchester Metropolitan University
Manchester, M1 5GD, UK

A. J. Chamkha
Department of Mechanical Engineering, Kuwait University
Safat-13060, Kuwait

G. Nath
Department of Mathematics, Indian Institute of Science
Bangalore-560012, India

2 Analysis

Let us consider a vertical heated flat surface with constant wall temperature T_w moving with constant velocity U in the x-direction, in a stable thermally stratified ambient fluid. The ambient temperature $T_\infty(x)$ is assumed to vary linearly with the height x. The buoyancy force arises due to the temperature differences in the fluid. We choose a rectangular Cartesian coordinate system with its origin fixed at the leading edge of the vertical surface, such that

the x-axis is directed upwards along the wall and the y-axis is measured normal to the surface, going into the fluid (see Fig. 1). Under the foregoing assumptions, the boundary layer equations with the Boussinesq approximations governing the flow and heat transfer on a continuously moving surface are given by [2, 4, 8, 14, 22];

$$u_x + v_y = 0 \tag{1}$$

$$u\,u_x + v\,u_y = g\beta(T - T_\infty) + \nu\,u_{yy} \ , \tag{2}$$

$$u\,T_x + v\,T_y = \alpha\,T_{yy} \ , \tag{3}$$

where

$$T_\infty(x) = T_0 + ax, \quad a = \mathrm{d}T_\infty/\mathrm{d}x > 0 \ . \tag{4}$$

The boundary conditions are given by;

$$\begin{aligned} &u(x,0) = U, \quad v(x,0) = 0, \quad T(x,0) = T_w, \\ &u(x,\infty) = 0, \quad T(x,\infty) = T_\infty(x), \\ &u(0,y) = 0, \quad T(0,y) = T_\infty(x), \quad y > 0 \ . \end{aligned} \tag{5}$$

Here u and v are the velocity components in the x and y directions, T is the temperature, g is the acceleration due to gravity, U is the wall velocity, β is the coefficient of thermal expansion, ν is the kinematic viscosity, α is the thermal diffusivity, T_0 is the ambient temperature at $x = 0$, a is the stratification rate of the slope of the ambient temperature profile with the vertical distance x taken as a constant in this study, and $a > 0$ implies that the ambient fluid is stably stratified, the subscripts w and ∞ denote conditions at the wall and in the ambient fluid, and the subscripts x and y denote derivative with respect to x and y.

In order to make Eqs. (1)–(3) dimensionless, we apply the following transformations;

$$\begin{aligned} &\eta = (U/\nu x)^{1/2} y, \quad \xi = x/L, \quad \psi(x,y) = (\nu x U)^{1/2} f(\xi,\eta), \\ &\theta(\xi,\eta) = (T(x,y) - T_\infty(x))/(T_w - T_0), \quad T_w - T_0 > 0, \\ &S = aL/(T_w - T_0) > 0, \quad \mathrm{Gr} = g\beta(T_w - T_0)L^3/\nu^2, \\ &\mathrm{Re} = UL/\nu, \quad \lambda = \mathrm{Gr}/(\mathrm{Re})^2, \quad \mathrm{Pr} = \nu/\alpha \ , \end{aligned} \tag{6}$$

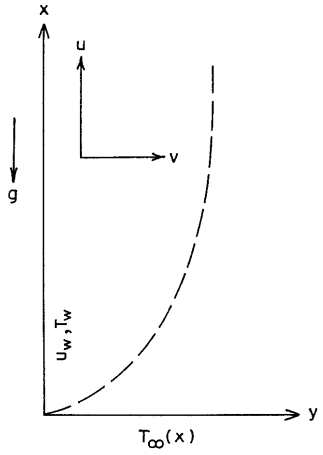

Fig. 1. Schematic diagram of the physical system

to the Eqs. (1)–(3) and we find that Eq. (1) is identically satisfied and the Eqs. (2) and (3) reduce to;

$$f''' + 2^{-1} f f'' + \lambda\xi\theta = \xi(f'\partial f'/\partial\xi - f''\partial f/\partial\xi) \ , \tag{7}$$

$$\theta'' + 2^{-1}\mathrm{Pr}\,f\theta' - S\,\mathrm{Pr}\,\xi f' = \mathrm{Pr}\,\xi(f'\partial\theta/\partial\xi - \theta'\partial f/\partial\xi) \ . \tag{8}$$

The boundary conditions (5) can be re-written as;

$$\begin{aligned} &f(\xi,0) = 0, \quad f'(\xi,0) = 1, \quad \theta(\xi,0) = 1 - S\xi, \\ &f'(\xi,\infty) = \theta(\xi,\infty) = 0 \ . \end{aligned} \tag{9}$$

Here η and ξ are the transformed coordinates, ψ and f are the dimensional and dimensionless stream functions, θ is the dimensionless temperature, L is the characteristic length, S is the dimensionless stratification parameter, Gr and Re are the global Grashof number and Reynolds number, λ is the buoyancy parameters, and $\lambda > 0$ for $T_w > T_0$, Pr is the Prandtl number, and prime denotes derivative with respect to η.

It may be remarked that for $S = 0$ (without stratification), $\lambda = 0$ (without buoyancy force) and $\xi = 0$ (self-similar flow), Eqs. (7)–(9) are the same as those of Erickson et al. [6] and Tsou et al. [8]. Also Eqs. (7)–(8) for $S = 0$ are identical to those of Moutsoglou and Chen [22] if we replace $\lambda\xi$ by ξ_1.

The skin friction coefficient C_{fx} and the heat transfer coefficient in terms of the Nusselt number Nu_x, can be expressed as;

$$C_{fx} = -2\mu(\partial u/\partial y)_{y=0}/\rho U^2 = -2\,\mathrm{Re}_x^{1/2} f''(\xi,0) \ , \tag{10a}$$

$$\mathrm{Nu}_x = -x(\partial T/\partial y)_{y=0}/(T_w - T_w) = -\mathrm{Re}_x^{-1/2}\theta'(\xi,0) \ , \tag{10b}$$

where μ is the coefficient of viscosity and $\mathrm{Re}_x(=Ux/\nu)$ is the local Reynolds number.

3
Method of solution

The partial differential Eqs. (7) and (8) under the boundary conditions (9) have been solved by using an implicit, iterative tridiagonal finite difference scheme similar to that of Blotnner [24]. All the first-order derivative with respect to ξ are replaced by two-point backward difference formulae;

$$\partial R/\partial\xi = (R_{i,j} - R_{i-1,j})/\Delta\xi \ , \tag{11}$$

where R is any dependent variable and i and j are the node locations along the ξ and η directions, respectively. First the third-order partial differential Eq. (7) is converted into a second-order by substituting $F = f'$. Then the second-order partial differential equations for F and θ are discretized by using three-point central difference formulae and all the first-order partial differential equations are discretized by employing the trapezoidal rule. At each time-step of constant ξ, a system of algebraic equations are solved iteratively by using the well-known Thomas algorithm (see Blotnner [24]). The same process is repeated for the next ξ value and the equations are solved line by line

until the desired ξ value is reached. A convergence criterion based on the relative difference between the current and previous iterations is used. When this difference reaches 10^{-5}, the solution is assumed to have converged and the iterative process is terminated.

We have examined the effect of grid size $\Delta\eta$ and $\Delta\xi$ and the edge of the boundary layer η_∞ on the solution. The results presented here are independent of grid size and η_∞ at least up to the 4th decimal place.

4
Perturbation expansion procedure

It is also possible to solve Eqs. (7)–(9) by using a perturbation expansion procedure [25] in terms of the streamwise distance ξ. This method is valid for small values of ξ, but the range of validity of ξ can be increased by using the Shanks transformation [26]. This method gives good results and the advantage has that one has to solve a system of ordinary differential equations instead of the partial differential equations.

We have assumed a regular perturbation expansion for f and θ in powers of ξ;

$$f(\xi,\eta)=\sum_{n=0}^{\infty}\xi^n f_n(\eta);\ \theta(\xi,\eta)=\sum_{n=0}^{\infty}\xi^n\theta_n(\eta)\ . \tag{12}$$

Substituting relations (12) into Eqs. (7)–(9), equating coefficients of like powers of ξ and truncating the expansion at the nth term, we obtain for $n=0$;

$$f_0'''+2^{-1}f_0f_0''=0\ . \tag{13a}$$

$$\theta_0''+2^{-1}\mathrm{Pr}\,f_0\theta_0' \tag{13b}$$

$$\begin{aligned} &f_0=0,\quad f_0'=\theta_0=1\quad \text{at } \eta=0,\\ &f_0'=\theta_0=0\quad \text{as } \eta\to\infty\ . \end{aligned} \tag{13c}$$

For $n=1$, we obtain;

$$f_1'''+2^{-1}(f_0f_1''+f_0'f_1)+\lambda\theta_0=(f_0'f_1'-f_0''f_1)\ , \tag{14a}$$

$$\theta_1''+2^{-1}\mathrm{Pr}(f_0\theta_0'+\theta_0'f_1)-\mathrm{Pr}\,Sf_0'=\mathrm{Pr}(f_0'\theta_1-\theta_0'f_1)\ , \tag{14b}$$

$$\begin{aligned} &f_1=f_1'=0,\quad \theta_1=-S\quad \text{at } \eta=0,\\ &f_1'=\theta_1=0\quad \text{as } \eta\to\infty\ . \end{aligned} \tag{14c}$$

Similarly, for $n\geq 2$, we obtain;

$$f_n'''+2^{-1}\sum_{m=0}^{n}f_mf_{n-m}''+\lambda\theta_{n-1}=\sum_{m=0}^{n-1}(n-m)(f_m'f_{n-m}'-f_m''f_{n-m})\ , \tag{15a}$$

$$\theta_n''+2^{-1}\mathrm{Pr}\sum_{m=0}^{n}f_m\theta_{n-m}'-S\,\mathrm{Pr}\,f_{n-1}'=\mathrm{Pr}\sum_{m=0}^{n-1}(n-m)(f_m'\theta_{n-m}-\theta_m'f_{n-m})\ , \tag{15b}$$

$$\begin{aligned} &f_0=f_n'=\theta_0=0\quad \text{at } \eta=0,\\ &f_n'=\theta_n=0\quad \text{as } \eta\to\infty\ . \end{aligned} \tag{15c}$$

The zeroth-order approximation given by Eqs. (13) corresponds to the self-similar flow on a moving surface in an ambient fluid studied by Sakiadis [5] and Tsou et al. [8] and the solutions are well known. The subsequent order approximations are linear equations and were solved by using the method of superposition [27].

The quantities of physical interest are the skin friction coefficient C_{fx} and the Nusselt number Nu_x which are given by Eq. (10) and these are re-written as;

$$2^{-1}\mathrm{Re}_x^{1/2}C_{fx}=-f''(\xi,0)=-\sum_{n=0}^{\infty}\xi^n f_n''(0)\ , \tag{16a}$$

$$\mathrm{Re}_x^{1/2}\mathrm{Nu}_x=-\theta'(\xi,0)=-\sum_{n=0}^{\infty}\xi^n\theta_n'(0)\ . \tag{16b}$$

Equations (16) are valid for small values of ξ, but the convergence of the above series can significantly be improved by using the Shanks transformation [26] which is expressed as

$$e(H_n)=(H_{n+1}H_{n-1}-H_n^2)/(H_{n+1}+H_{n-1}-2H_n)\ , \tag{17}$$

where H_n is the partial sum of n terms of the series and e is the operator. Here we have taken $n=4$ and the above transformation is applied twice to Eq. (16). The results differ by less than 1% from the numerical results in the range $0\leq\xi\leq 1$.

5
Results and discussion

We have validated our results by comparing the velocity profile $(u/U=f')$ for $S=0$ (no stratification), $\lambda=0$ (no buoyancy force) and $\xi=0$ (self-similar case) with the theoretical and experimental results of Tsou et al. [8] in Fig. 2. We find that the velocity profile u/U is in very good agreement with the theoretical values. It also agrees well with the experimental values near the wall. Also we have compared the Nusselt number Nu_x, for $S=\xi=0$ with the theoretical value of Erickson et al. [6] and the experimental values of Griffin and Throne [7]. This comparison is shown in Fig. 3 and results are found to be in good agreement with the theoretical and experimental results,

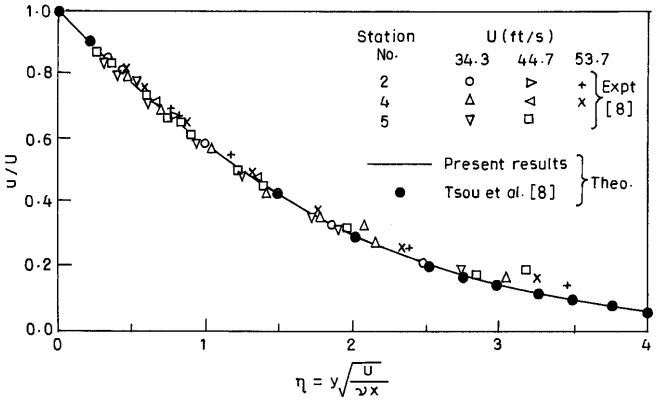

Fig. 2. Comparison of the velocity profile u/U for $S=\lambda=\xi=0$ with that of Tsou et al. [8]

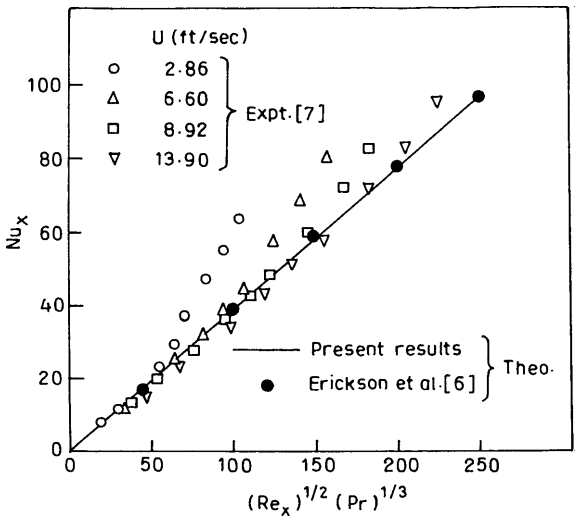

Fig. 3. Comparison of the Nusselt number Nu_x for $S = \lambda = \xi = 0$ with that of Erickson et al. [6] and Griffin and Throne [7]

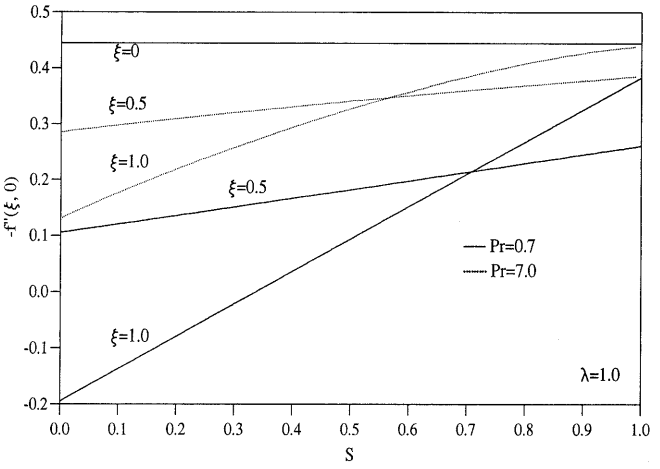

Fig. 4. Effect of the thermal stratification parameter S on the surface shear stress $-f''(\xi, 0)$

when the wall velocity $U \geq 8.92$. Further, we have compared the values of the surface shear stress $(f''(\xi, 0))$ and the surface heat transfer $(-\theta/(\xi, 0))$ for $S = 0$ with those of Moutsoglou and Chen [22]. For direct comparison we have to replace $\lambda\xi$ by ξ_1 and hence $\xi\partial/\partial\xi = \xi_1\partial/\partial\xi_1$. The results are in excellent agreement. The comparison is presented in Table 1. Here we have considered the natural convection flow over a vertical surface moving with constant velocity in a thermally stratified medium. This problem is different from that over a stationary surface studied in references [1–4]. Hence it is not possible to compare our results with those given in [1–4].

The effect of the ambient thermal stratification parameter S on the surface shear stress $-f''(\xi, 0)$ at three locations downstream of the leading edge of the surface (i.e., for three values of ξ) and for two values of the Prandtl number Pr is shown in Fig. 4. An increase in the thermal stratification parameter S tends to reduce the velocity and the boundary layer thickness (slightly) which is evident from Fig. 4. Consequently, the velocity gradient is increased and hence the surface shear stress $-f''(\xi, 0)$ is increased. The effect of the stratification parameter S is more pronounced for lower values of the Prandtl number Pr. For $\xi = 0.5$, $\lambda = 1$, the surface shear stress $-f''(\xi, 0)$ increases by about 143% as S increases from 0 to 1 when Pr = 0.7 and by about 57% when Pr = 7. It may be noted that $f''(\xi, 0) < 0$ implies that the fluid near the wall is being dragged by the moving wall and $f''(\xi, 0) > 0$ implies that the plate is being dragged by the fluid. Hence the vanishing of the surface shear stress $f''(\xi, 0)$ does not imply separation [22]. Since the stratification parameter S is multiplied by ξ (see Eqs. (7)–(9)), it has no effect at the leading edge of the plate (i.e., at $\xi = 0$). For $\lambda = 1$, $\xi < 0.6625$ and $\mathrm{Pr} \geq 0.7$, $f''(\xi, 0) < 0$ for all values of S in the range of $(0 \leq S \leq 1)$, but for $\xi > 0.6625$, $f''(\xi, 0) > 0$ for some values of S. For example, for $\xi = \lambda = 1$, $\mathrm{Pr} = 0.7$, $f''(\xi, 0) > 0$ for $S < 0.32$ and $f''(\xi, 0) < 0$ for $S > 0.32$. For fixed values of ξ, S and λ, the surface shear stress $-f''(\xi, 0)$ increases with the Prandtl number Pr due to the reduction in the momentum boundary layer. For $S = \lambda = 1$, $\xi = 0.5$, $-f''(\xi, 0)$ increases by about 49% as Pr increases from 0.7 to 7.

Figure 5 presents the effect of the stratification parameter S on the surface heat transfer $-\theta'(\xi, 0)$ for three values of ξ and two values of Pr when the buoyancy parameter $\lambda = 1$. As mentioned earlier, there is no effect of S at the leading edge of surface $(\xi = 0)$ as is evident from Eqs. (7)–(9). It is observed that the surface heat transfer $-\theta'(\xi, 0)$

Table 1. Comparison of the surface shear stress $f''(\xi_1,0)$ and the surface heat transfer $-\theta'(\xi_1, 0)$ for $S = 0$ with those of Moutsoglou and Chen [22]

ξ_1	Present results				Moutsouglou and Chen			
	Pr = 0.7		Pr = 7.0		Pr = 0.7		Pr = 7.0	
	$f''(\xi_1, 0)$	$-\theta'(\xi_1, 0)$	$f''(\xi_1, 0)$	$-\theta'(\xi_1, 0)$	$f''(\xi_1, 0)$	$-\theta'(\xi_1, 0)$	$f''(\xi_1, 0)$	$-\theta'(\xi_1, 0)$
0	−0.44372	0.34922	−0.44372	1.38698	−0.44375	0.34924	−0.44375	1.38703
0.5	−0.10556	0.41317	−0.28373	1.41317	−0.10558	0.41320	−0.28376	1.41322
1.0	0.19423	0.45502	−0.12874	1.43706	0.19425	0.45505	−0.12876	1.43712
1.5	0.47217	0.47761	0.02107	1.45932	0.47214	0.47764	0.02105	1.45938
2.0	0.73556	0.50035	0.16883	1.48032	0.73552	0.50031	0.16880	1.48026
3.0	1.23107	0.53685	0.45321	1.53647	1.23103	0.53681	0.45318	1.53641
4.0	1.69657	0.56613	0.72694	1.55340	1.69652	0.56609	0.72697	1.55334
5.0	2.13993	0.59090	0.99207	1.58517	2.13988	0.59086	0.99201	1.58510

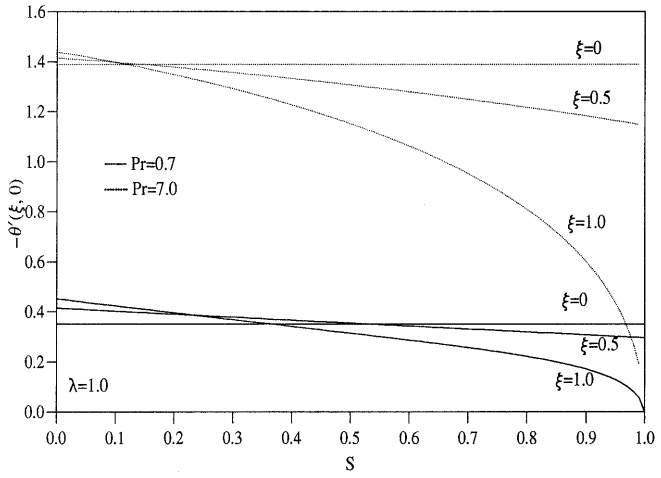

Fig. 5. Effect of thermal stratification parameter S on the surface heat transfer $-\theta'(\xi,0)$

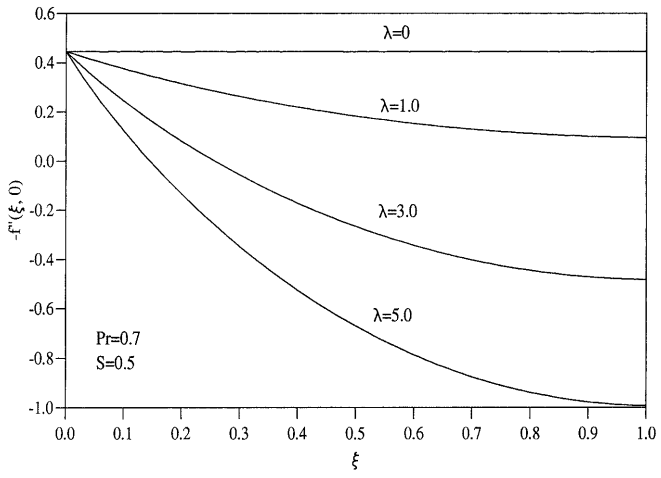

Fig. 6. Effect of the buoyancy parameter λ on the surface shear stress $-f''(\xi,0)$

reduces with increasing values of S. The effect of the stratification becomes more pronounced with increasing ξ, because S is multiplied by ξ (see Eqs. (8) and (9)). For $\lambda = \xi = 1$, Pr = 7.0, the surface heat transfer $-\theta'(\xi,0)$ decreases by 100% as the value of S increases from 0 to 1. The reason for the reduction in the surface heat transfer is that the temperature decreases with an increasing stratification parameter S (see Fig. 9). Hence the temperature gradient at the wall decreases and the surface heat transfer also decreases. For fixed values of S, λ and ξ, the surface heat transfer $-\theta'(\xi,0)$ increases with the Prandtl number Pr due to significant reduction in the thermal boundary layer thickness. The reason for the strong dependence of the surface heat transfer on Pr is that Pr occurs explicitly in the energy equation (see Eq. (8)). For $S = \lambda = 1$, $\xi = 0.5$, the surface heat transfer $-\theta(\xi,0)$ increases by about 27% as Pr increases from 0.7 to 7.

The effect of the buoyancy parameter λ on the surface shear stress $-f''(\xi,0)$ for $0 \leq \xi \leq 1$, $S = 0.5$ and Pr = 0.7 is displayed in Fig. 6. The surface shear stress $f''(\xi,0)$ increases very significantly with the buoyancy parameter due to the significant reduction in the boundary layer thickness caused by the increase in the buoyancy force, which acts like a favourable pressure gradient. For $\xi = 1$, $S = 0.5$, Pr = 0.7, the surface shear stress increases by about 300% as λ increases of 0 to 5. The reason for the strong dependence of the shear stress on the buoyancy parameter λ is that it occurs explicitly in the momentum equation (see Eq. (7)). Also the surface shear stress changes significantly with the streamwise distance ξ for large values of the buoyancy parameter λ, because λ is multiplied by ξ (see Eq. (7)). For $\lambda = 5$, Pr = 0.7, $S = 0.5$, $f''(\xi,0)$ decreases by about 270% as ξ increases from 0 to 1. For $\lambda < 1.21$, Pr = 0.7, $S = 0$, $f''(\xi) < 0$ for all values of ξ in $0 \leq \xi \leq 1$. For $\lambda > 1.21$, $f''(\xi,0) > 0$ for some locations of ξ. The significance of $f''(\xi,0) \gtrless 0$ has been explained earlier. The reason for this trend is that the positive buoyancy force ($\lambda > 0$) acts like a favourable pressure gradient and accelerates the fluid motion. Consequently, as λ increases beyond a certain value, the velocity of the fluid near the wall exceeds the velocity at the surface. Hence the velocity gradient and the surface shear stress become positive.

The effect of the buoyancy parameter λ on the surface heat transfer for $0 \leq \xi \leq 1$, Pr = 0.7, $S = 0.5$ is presented in Fig. 7. For $\xi > 0$, the surface heat transfer $-\theta'(\xi,0)$ increases with the buoyancy parameter λ due to the reduction in the thermal boundary layer thickness (see Fig. 7). For $\xi = 1$, $S = 0.5$, Pr = 0.7, the surface heat transfer $\theta'(\xi,0)$ increases by about 81% as λ increases from 0 to 5. Also for $\lambda > 0.32$, $\theta'(\xi,0)$ first increases with ξ, and then decreases. However, for $\lambda \leq 0.32$, it continuously decreases as ξ increases.

The effect of the thermal stratification parameter S on the velocity and temperature profiles $(f'(\xi,\eta), \theta(\xi,\theta))$ for $\lambda = 1$, $\xi = 0.5$, Pr = 0.7 is shown in Figs. 8 and 9. The effect of S on the temperature profiles is found to be more pronounced than that on the velocity profiles, because S occurs explicitly in the equation as well as in the boundary conditions for temperature θ (see Eqs. (8) and (9)), whereas the effect of S on the velocity profiles $f'(\xi,\eta)$ is indirect. Both velocity and temperature profiles $f'(\xi,\eta)$,

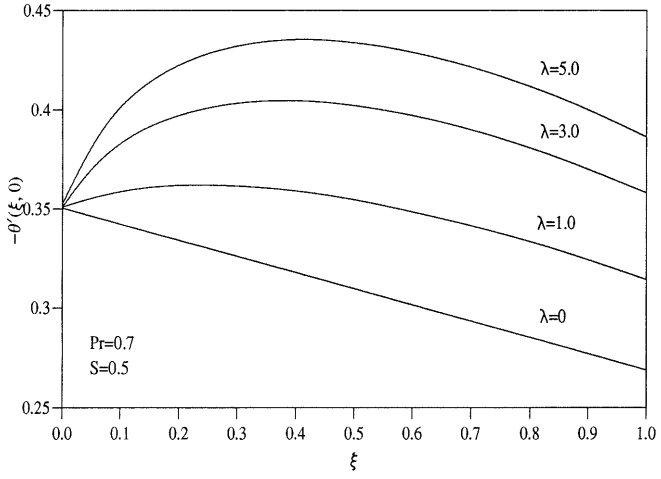

Fig. 7. Effect of the buoyancy parameter λ on the surface heat transfer $-\theta'(\xi,0)$

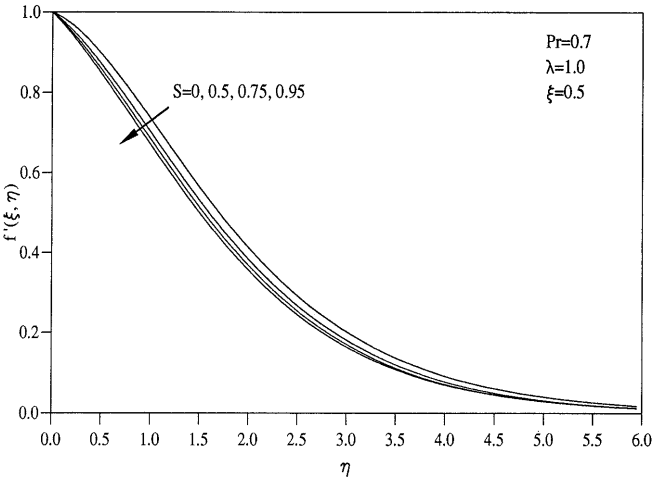

Fig. 8. Effect of the thermal stratification parameter S on the velocity profiles $-f'(\xi,\eta)$

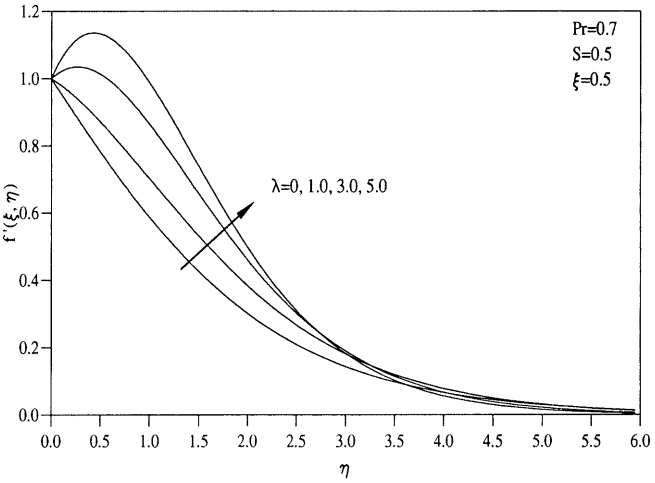

Fig. 10. Effect of the buoyancy parameter λ on the velocity profiles $f'(\xi,\eta)$

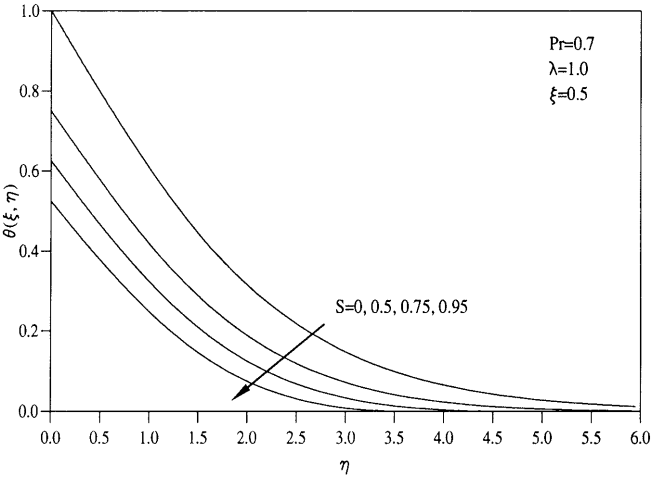

Fig. 9. Effect of the thermal stratification parameter S on the temperature profiles $\theta(\xi,\eta)$

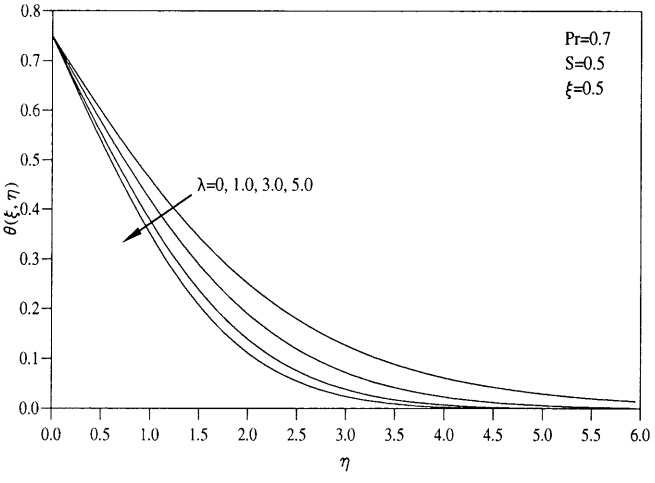

Fig. 11. Effect of the buoyancy parameter λ on the temperature profiles $\theta(\xi,\eta)$

$\theta(\xi,\eta)$ decrease with increasing S. The thermal boundary layer is found to be thinner than the momentum boundary layer. Further the temperature on the wall $(\theta(\xi,0))$ decreases by about 48% as S increases from 0 to 0.95.

Figures 10 and 11 present the effect of buoyancy parameter λ on the velocity and temperature profiles $f'(\xi,\eta)$, $\theta(\xi,\eta)$ for $S=\xi=0.5$, and Pr = 0.7. Since the positive buoyancy parameter λ acts like a favourable pressure gradient, it increases the velocity and causes an overshoot in the velocity near the wall when λ exceeds a certain value. Similar trend was observed Moutsoglou and Chen [22] for $S=0$ (without stratification). For $\xi=S=0.5$, Pr = 0.7, the velocity overshoot occurs for $\lambda>2.26$ and for $\lambda=5$, the velocity overshoot is about 14%. The thermal boundary layer decreases with increasing λ.

The effect of Prandtl number Pr on the velocity and temperature profiles $(f'(\xi,\eta),\theta(\xi,\eta))$ for $\lambda=1$, $S=\xi=0.5$ is shown in Figs. 12 and 13. The effect of Pr is more pronounced on the temperature profiles $\theta(\xi,\eta)$ than on the velocity profiles $(f'(\xi,\eta))$, because Pr occurs

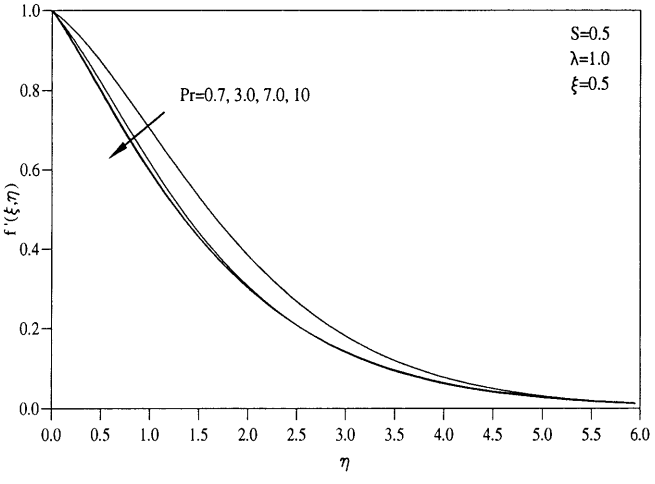

Fig. 12. Effect of the Prandtl number Pr on the velocity profiles $f'(\xi,\eta)$

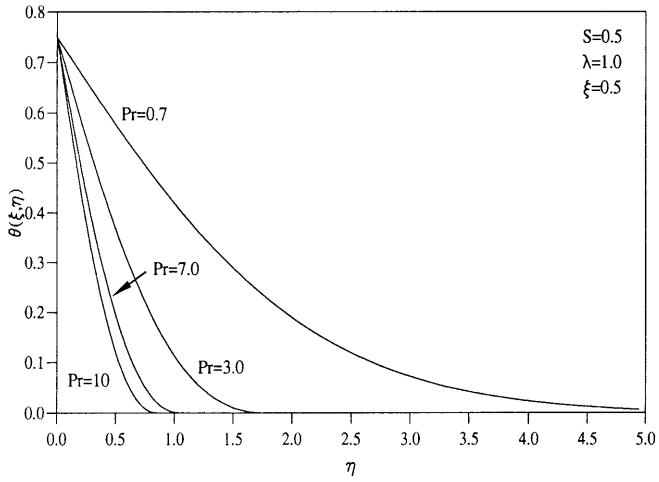

Fig. 13. Effect of the Prandtl number Pr on the temperature profiles $\theta(\xi, \eta)$

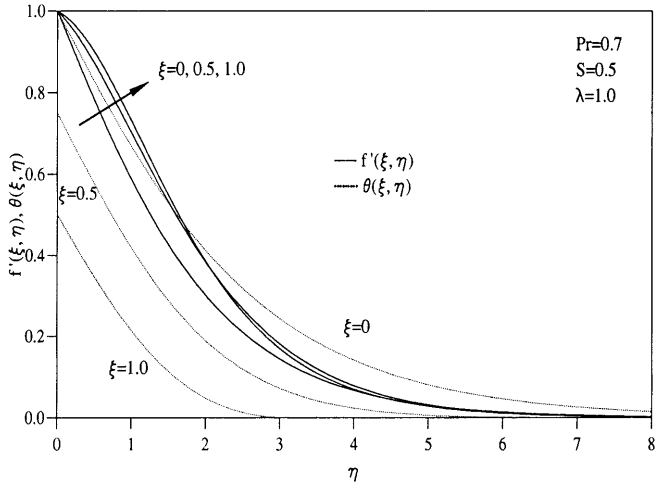

Fig. 14. Effect of the streamwise distance ξ on the velocity and the temperature profiles $f'(\xi, \eta)$, $\theta(\xi, \eta)$

explicitly in the energy equation (see Eq. (8)). The thermal boundary layer becomes considerably thinner with increasing Pr.

Figure 14 displays the effect of the streamwise distance ξ on the velocity and temperature profiles $f(\xi, \eta), \theta(\xi, \eta)$ for $\lambda = 1$, $S = 0.5$, Pr = 0.7. The temperature profiles $\theta(\xi, \eta)$ are strongly affected by ξ, whereas its effect on the velocity profiles $f'(\xi, \eta)$ is comparatively weak. Also the thermal boundary layer is found to be much thinner than the momentum boundary layer.

6 Conclusions

The thermal stratification significantly affects both the flow and the temperature fields. The surface shear stress, generally, increases with the thermal stratification, whereas the surface heat transfer decreases. For small values of the Prandtl number, the surface shear stress changes sign at a certain value of the stratification parameter. The buoyancy force and the Prandtl number significantly increase the surface shear stress and the surface heat transfer. The buoyancy force gives rise to an overshoot in the velocity profiles near the wall. Also for small values of the Prandtl number and for large streamwise distances, the surface shear stress changes very significantly. The results of the perturbation procedure used along with the Shanks transformation are in very good agreement with those obtained by using the numerical method.

References

1. **Eichhorn R** (1969) Natural convection in a thermally stratified fluid. Prog Heat Mass Transfer 2: 41–58
2. **Chen CC; Eichhorn R** (1976) Natural convection from a vertical surface to a thermally stratified fluid. J Heat Transfer 98: 446–451
3. **Venkatachala BJ; Nath G** (1981) Non-similar laminar natural convection in a thermally stratified fluid. Int J Heat Mass Transfer 24: 1848–1859
4. **Kulkarni AK; Jacob HR; Hwang JJ** (1987) Similarity solution for natural convection flow over an isothermal vertical wall immersed in a thermally stratified medium. Int J Heat Mass Transfer 30: 691–698
5. **Sakiadis BC** (1961) Boundary layer behaviour on continuous solid surface. II, The boundary layer on a continuous flat surface. AIChE J 7: 221–225
6. **Erickson LE; Fan LT; Fox VG** (1966) Heat and mass transfer on a moving continuous flat plate with suction or blowing. Ind Eng Chem Fund 5: 19–25
7. **Griffin JF; Throne JL** (1967) On the thermal boundary layer growth on continuous moving belts. AIChE J 13: 1210–1211
8. **Tsou FK; Sparrow EM; Goldstein RJ** (1967) Flow and heat transfer in the boundary layer on a continuously moving surface. Int J Heat Mass Transfer 10: 219–235
9. **Crane LJ** (1970) Flow past a stretching plate. ZAM P 21: 445–447
10. **Gupta PS; Gupta AS** (1977) Heat and mass transfer on a stretching sheet with suction or blowing. Cand J Chem Eng 55: 744–746
11. **Chakrabarti A; Gupta AS** (1979) Hydromagnetic flow, heat and mass transfer over a stretching sheet. Quart Appl Math 33: 73–78
12. **Carragher P; Crane LJ** (1982) Heat transfer on a continuously moving sheet. ZAMM 62: 564–565
13. **Dutta BK; Roy P; Gupta AS** (1985) Temperature field in flow over a stretching sheet with uniform heat flux. Int Comm Heat Mass Transfer 28: 1234–1237
14. **Jeng DR; Chang TCA; Dewitt KJ** (1986) Momentum and heat transfer on a continuous moving surface. ASME J Heat Transfer 108: 532–537
15. **Dutta BK** (1989) Heat transfer from a stretching sheet with uniform suction or blowing. Acta Mechanica 78: 255–262
16. **Chappadi PR, Gunnerson PS** (1989) Analysis of heat and momentum transport along a moving surface. Int J Heat Mass Transfer 32: 1383–1386
17. **Chiam TC** (1993) Magnetohydrodynamic boundary layer flow due to a continuously moving plate. Computer Math Applics 26: 1–7
18. **Lin HT; Huang SF** (1994) Flow and heat transfer of plane surface moving in parallel and reversely in the free stream. Int J Heat Mass Transfer 37: 333–336
19. **Andersson HJ** (1995) An exact solution of the Navier–Stokes equations for MHD flow. Acta Mechanica 113: 241–244
20. **Chiam TC** (1996) Heat transfer with variable conductivity in a stagnation-point flow towards a stretching sheet. Int Comm Heat Mass Transfer 23: 239–248
21. **Vajravelu K; Hadjinicolaou A** (1997) Convective heat transfer in an electrically conducting fluid at a stretching surface with uniform free stream. Int J Eng Sci 35: 1237–1244

22. **Moutsoglou A;. Chen TS** (1980) Buoyancy effects in boundary layers on inclined continuous moving sheets. ASME J Heat Transfer 102: 171–173
23. **Ramachandran N; Armaly BF; Chen TS** (1987) Correlation for laminar mixed convection in boundary layer adjacent to inclined continuous moving sheets. Int J Heat Mass Transfer 30: 2196–2199
24. **Blotnner FG** (1970) Finite-difference method of solution of the boundary layer equations. AIAA J 8: 193–205
25. **Aziz A; Na TY** (1982) An improved perturbation solution for laminar natural convection on a vertical cylinder. Warme- und Stoffubertragung 10: 83–87
26. **Shanks D** (1955) Nonlinear transformations of divergent and slowly convergent sequences. J Math Phys 34: 1–42
27. **Na TY** (1979) Computational Methods in Engineering Boundary Value Problems. Academic Press, New York